

# Stellae Octangulae in Motion Revisited

## Stellae Octangulae in Motion Revisited

### ABSTRACT

It is well-known that two congruent regular tetrahedra  $T_1$  and  $T_2$  forming a Stella Octangula allow a continuous motion of  $T_2$  relative to  $T_1$  such that each edge of  $T_2$  slides along an edge of  $T_1$ . Recently the same property has been confirmed for pairs  $(T_1, T_2)$  of indirect congruent tetrahedra of general form. It turns out that this overconstrained kinematical systems admits besides some special one-parameter motions also two-parameter motions. We provide a synthetic analysis of the problem. Based on involved quadrics, we study in depth the two-parameter motions and their boundaries. Moreover, we present some generalizations of Stellae Octangulae.

**Key words:** tetrahedron, Stella Octangula, Euclidean motion, two-parameter movements

**MSC2020:** 51N20, 51N30

## Zvjezdasti oktaedari (Stellae Octangulae) u pokretu – ponovno razmatranje

### SAŽETAK

Dobro je poznato da dva tetraedra  $T_1$  i  $T_2$  koji tvore zvjezdasti oktaedar (Stella Octangula) dopuštaju neprekidno gibanje tetraedra  $T_2$  s obzirom na tetraedar  $T_1$  takvo da svaki brid tetraedra  $T_2$  klizi duž brida tetraedra  $T_1$ . Nedavno je isto svojstvo potvrđeno za parove  $(T_1, T_2)$  indirektno sukladnih tetraedara općeg oblika. Pokazuje se da taj prenapregnuti kinematički sustav, osim nekih posebnih jednoparametarskih gibanja, dopušta i dvoparametarska gibanja. Dajemo sintetičku analizu problema. Na temelju uključenih kvadrika detaljno proučavamo dvoparametarska gibanja i njihove granice. Osim toga, predstavljamo neka poopćenja zvjezdastih oktaedara.

**Ključne riječi:** tetraedar, zvjezdasti oktaedar (Stella Octangula), euklidsko gibanje, dvoparametarski pomaci

## 1 Introduction

As reported in [8], during the assembly of a physical model of the classical Stella Octangula in 1982, L. Tompos Jr. discovered the relative movability of two regular tetrahedra  $T_1, T_2$  with permanent edge-contacts. Note that at this physical model one tetrahedron encloses the other, and the exterior tetrahedron consists of edges only (Figure 1).

Though generically six edge-contacts fix the pose of one tetrahedron relative to the other, in the case of regular tetrahedra  $T_1, T_2$  one tetrahedron can slide along the other such that each edge of  $T_1$  keeps contact with an edge of  $T_2$ . According to [11] in 1988, this overconstrained kinematic structure admits four one-parameter motions and three two-parameter motions that all share the initial Stella-Octangula pose.

Later the question arose, whether the regular Stella Octangula is the only one with movable tetrahedral parts. Answers were given in [8, 12, 13]: Starting with a generalized

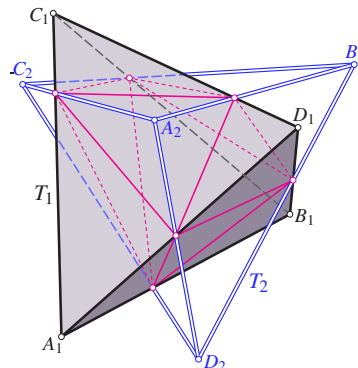


Figure 1: Two congruent regular tetrahedra  $T_1$  and  $T_2$  with crossing edges, i.e., with six edge-contacts. The magenta lines represent the octahedron  $O = T_1 \cap T_2$

Stella Octangula consisting of congruent tetrahedra  $T_1$  and  $T_2$ , one was looking for an at least one-parameter motion of  $T_2$  relative to  $T_1$ , where the six edge-contacts are preserved.

In [8], the authors describe analytically six distinct types of such constrained motions in the case where the convex hull of the Stella Octangula is a box, i.e., a rectangular parallelepiped. Most of these motions are rotations about axes in particular position relative to the given box.

Below we present a synthetic approach, where one-sheeted hyperboloids of revolution and orthogonal hyperbolic paraboloids play an essential role. After discussing some basic properties of such pairs of tetrahedra, we analyse in the Sections 3 and 4 two special cases, namely two congruent right three-sided pyramids and, in alignment with [8], equifacial tetrahedra. As main topic, we focus in Sections 5 to 6 on generic tetrahedra  $T_1$  and their indirect congruent copies  $T_2$ . For tetrahedra with acute-angled faces and others, there exist even two-parameter motions of  $T_2$  against  $T_1$  that preserve all edge-contacts. We study necessary and sufficient conditions and the boundaries of these motions. Moreover, we describe included one-parameter movements where all points' trajectories are located in parallel planes. Similar to the generalizations presented in [8], we finally provide in Section 7 further examples.

## 2 Basic properties of two tetrahedra with six edge-contacts

For the sake of simplicity, we introduce the following notation.

**Definition 1** *Two tetrahedra  $T_1$  and  $T_2$  are said to have crossing edges, if they have six mutual edge-contacts and each contact point is an interior point of both involved edges.*

With regard to a generalization of the cube circumscribed to a regular Stella Octangula, we can state:

**Lemma 1** *Two tetrahedra  $T_1$  and  $T_2$  have crossing edges if and only if their convex hull  $\mathcal{H}$  is a convex cuboid, i.e., a hexahedron with six quadrangular faces.*

**Proof.** The vertices of two tetrahedra  $T_1, T_2$  with crossing edges are already the eight vertices of their convex hull  $\mathcal{H}$ . Each of the six faces of  $\mathcal{H}$  has a pair of intersecting edges as diagonals.

Conversely, the two tetrahedra  $T_1, T_2$  arise by truncating the cuboid  $\mathcal{H}$  in the way that the edges of the tetrahedra are diagonals of the faces of  $\mathcal{H}$ . At a convex cuboid each quadrangular face is convex, too, so that the point of intersection between the two diagonals is an interior point of the edges, as required in Definition 1.  $\square$

The following lemma can be seen as a dual counterpart.

**Lemma 2** *If two tetrahedra  $T_1$  and  $T_2$  have crossing edges, then the intersection of the solids  $O := (T_1 \cap T_2)$  is a convex octahedron. Conversely, each convex octahedron  $O$  is the intersection of two tetrahedra with crossing edges, but not all tetrahedral vertices need to be finite.*

**Proof.** The intersection  $O$  of the two convex solids  $T_1$  and  $T_2$  must be convex, too. Each of the eight faces of  $T_1$  or  $T_2$  intersects the other tetrahedron along a triangle with vertices at the coplanar contact points. Thus, the six contact points are the vertices of  $O$  (see Figure 1).

Conversely, the eight bounding planes of any convex octahedron  $O$  can be separated into two quadruples such that any two planes  $\varepsilon, \varphi$  of the same quadruple contain octahedral faces that share exactly one vertex. The line  $\varepsilon \cap \varphi$  must be a (proper) support line of  $O$ , i.e., it meets  $O$  only at a single point since otherwise, due to the convexity of  $O$ , the octahedral faces in  $\varepsilon$  and  $\varphi$  would share a line segment. Each bounding plane  $\varepsilon$  contains a triangular face of  $O$ . Let us assume that the four planes of the quadruple through  $\varepsilon$  have a point  $P$  in common. Then  $\varepsilon$  intersects the three remaining planes along lines that connect  $P$  with the coplanar vertices of  $O$ . At least one of them cannot be a (proper) support line of  $O$  as it meets the closed triangular face along a line segment. This contradiction with our assumption reveals, that each quadruple defines a tetrahedron, provided that also vertices at infinity are admitted.  $\square$

### 2.1 A kinematic analysis

Suppose that  $T_1$  and  $T_2$  are two tetrahedra with crossing edges. Each single edge-contact reduces the degree of freedom ('dof', for short) of  $T_2$  relative to  $T_1$  by 1. Therefore, the Chebychev-Grübler-Kutzbach formula yields  $\text{dof} = 0$ . In other words,  $T_1$  is generically rigid relative to  $T_2$ . The following kinematical statement shows that in general  $T_1$  is even infinitesimally rigid relative to  $T_2$ .

**Theorem 1** *Given two tetrahedra  $T_1, T_2$  with crossing edges, let  $P_i$  for  $i = 1, \dots, 6$  be the six points where an edge  $e_{i1}$  of  $T_1$  meets an edge  $e_{i2} \subset T_2$ . Then  $T_2$  is infinitesimally movable relative to  $T_1$  if and only if the six perpendiculars  $n_i$  through  $P_i$  to the planes spanned by  $e_{i1}$  and  $e_{i2}$  belong to a linear complex of lines.*

**Remark 1** *By virtue of Lemma 1, the contact points  $P_i$  are the crossing points of the diagonals in the quadrangular faces of the convex hull  $\mathcal{H}$ , and the normals  $n_i$  at  $P_i$  are orthogonal to the faces.*

**Proof.** The tetrahedron  $T_2$  is *infinitesimally movable* relative to  $T_1$ , if and only if one can assign to each point attached to  $T_2$  a velocity vector such that for any two points  $X, Y$  their mutual distance remains infinitesimally constant, i.e., for the respectively assigned velocity vectors  $\mathbf{v}_X, \mathbf{v}_Y$  the difference vector  $\mathbf{v}_X - \mathbf{v}_Y$  is perpendicular to the line  $XY$ .<sup>1</sup> This is equivalent to the statement that for all points  $X$  in space the lines through  $X$  orthogonal to  $\mathbf{v}_X$  belong to a linear complex of lines (see, e.g., [1, p. 162] [3, p. 292] or [6, p. 219]). The axis of this linear complex coincides with the instantaneous screw axis of the motion of  $T_2$  against  $T_1$ .

Suppose that there exists such an infinitesimal motion of  $T_2$  relative to  $T_1$ . Then, in order to preserve the edge-contact between  $e_{i1}$  and  $e_{i2}$ , the velocity vector  $\mathbf{v}_i^r$  of the point of contact  $P_i$  relative to  $T_2$  must be parallel to  $e_{i2}$ , while relative to  $T_1$  the velocity vector  $\mathbf{v}_i^a$  of  $P_i$  is parallel to  $e_{i1}$ . The edge-contacts preserving motion of  $T_2/T_1$  assigns to  $P_i$  the velocity  $\mathbf{v}_{P_i} = \mathbf{v}_i^a - \mathbf{v}_i^r$  ('absolute' minus 'relative') parallel to the plane connecting  $e_{i1}$  with  $e_{i2}$ . Consequently, the line  $n_i$  through  $P_i$  and orthogonal to  $e_{i1}$  and  $e_{i2}$  belongs to the linear complex of path-normals. This argumentation works also in the converse direction.  $\square$

It needs to be noted that the characterization presented in Theorem 1 makes no difference whether the meeting point between  $e_{i1}$  and  $e_{i2}$  lies on the edges or outside on the extending lines.

**Remark 2** Referring to Theorem 1, let the set of linear line complexes through the six perpendiculars  $n_i$ ,  $i = 1, \dots, 6$ , be one- or two-dimensional. Then the local dof of infinitesimal motions of  $T_2$  relative to  $T_1$  equals two or three.

If  $T_2$  is continuously movable against  $T_1$  like in the regular case, then it is infinitesimally movable in each pose. In particular, in the regular Stella-Octangula pose, the six path normals  $n_1, \dots, n_6$  coincide with three mutually orthogonal diameters of a regular octahedron  $O$ . This implies that even each infinitesimal spherical motion of  $T_2$  about the common center  $O$  preserves all edge-contacts with  $T_1$  since  $\mathbf{v}_O = \mathbf{0}$ .

In the following sections we only focus on pairs of **congruent** tetrahedra  $(T_1, T_2)$  with crossing edges. This means that in each pose of  $T_2$  relative to  $T_1$  there is a displacement  $\alpha: T_1 \rightarrow T_2$ . We recall from the classification of congruences in the Euclidean 3-space (see, e.g., [10]): If  $\alpha$  is orientation preserving, then it is either a translation or a rotation or screw motion. Otherwise,  $\alpha$  is either a reflection in a plane  $\sigma$  or the commutative product of this reflection with a translation parallel to  $\sigma$  or with a rotation about an axis orthogonal to  $\sigma$ . The only involutive displacements are reflections in a point, in a line or in a plane; only the second one is orientation preserving.

### 3 Stellae Octangulae formed by right three-sided pyramids

Let  $T_1$  and  $T_2$  be two congruent right three-sided pyramids in a Stella-Octangula position, i.e., with edge-contacts at all midpoints of edges (Figure 2, top). Then there exists a one-parameter motion with permanent edge-contacts while the axes of rotational symmetry are coinciding in the line  $a$  which is supposed to be vertical. This mobility arises from the case of regular tetrahedra treated in [11] by an affine transformation, an appropriate scaling along the axis  $a$ . But this time we move simultaneously both tetrahedra  $T_1$  and  $T_2$ , while the common axis  $a$  and two planes of symmetry between  $T_1$  and  $T_2$  remain fixed, namely one plane  $\varphi_0$  orthogonal to  $a$ , hence horizontal, and the other  $\varphi_1$  passing through  $a$ . Therewith, the two tetrahedra remain symmetric with respect to (w.r.t., for short) a fixed axis, the intersection  $s = \varphi_0 \cap \varphi_1$  of the two planes of symmetry (see Figure 3).

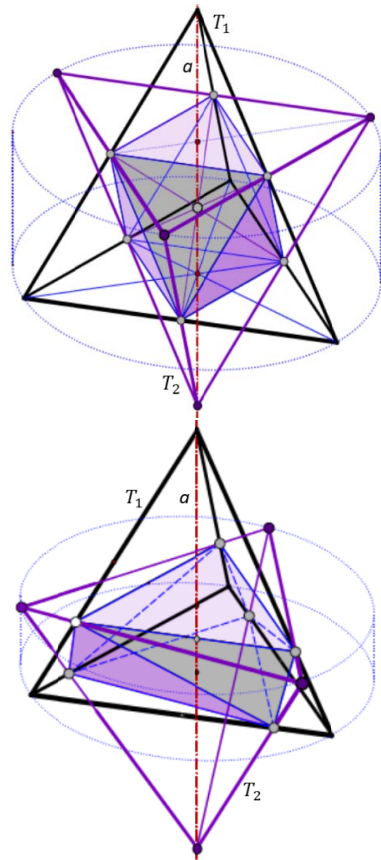


Figure 2: *Stella Octangula* consisting of two right tetrahedra  $T_1$  and  $T_2$  in the highly symmetric start position (top), and in an intermediate position (bottom).

<sup>1</sup>Throughout the paper,  $XY$  denotes the line connecting the two points  $X$  and  $Y$ , while the symbol  $[XY]$  stands for the segment bounded by  $X$  and  $Y$ .

During this one-parameter motion, one vertex of each tetrahedron moves on the axis  $a$ , while the other vertices trace algebraic curves on a coaxial cylinder (see Figure 4). The octahedron  $O$  of contact points shows up in form of an antiprism with regular triangles as base and top face (see Figure 2, bottom). In the initial pose the six remaining faces are congruent isosceles triangles.

For a detailed analysis of the movements of the two pyramids we denote the vertices of the basis of  $T_i$  with  $A_i, B_i, C_i$  and the apex with  $D_i$ ,  $i = 1, 2$ . We introduce cylinder coordinates with the vertical altitude  $a$  as  $z$ -axis, with the origin  $O$  in the fixed plane  $\varphi_0$  and the zero-direction along  $s$  in the fixed plane  $\varphi_1$  and pointing to the right in Figure 3. The circumcircles of the base triangles of the two coaxial tetrahedra  $T_1$  and  $T_2$  are assumed as unit circles.

Let  $(1, \alpha, -h_\alpha)$  be the cylinder coordinates of  $A_1$  and  $(1, -\alpha, h_\alpha)$  that of  $A_2$ . Then, the point of intersection  $P_1$  between the edges  $[A_1 D_1]$  and  $[A_2 B_2]$  (see Figure 3) has coordinates  $(\rho, \alpha, h_\alpha)$ . The point of intersection  $Q = \varphi_0 \cap A_1 D_1$  gets – because of  $\overline{Q A_1} = \frac{1}{2}(1 - \rho) =: \bar{\rho}$  – the cylinder coordinates  $(1 - \bar{\rho}, \alpha, 0)$ , where

$$\rho = \frac{1}{2 \cos(\pi/3 - 2\alpha)}, \quad \bar{\rho} = \frac{\cos 2\alpha + \sqrt{3} \sin 2\alpha - 1}{2(\cos 2\alpha + \sqrt{3} \sin 2\alpha)}, \quad \text{for } 0 \leq \alpha \leq \pi/3. \quad (1)$$

The choice  $\alpha = \pi/6$  yields the Stella-Octangula position. For  $\alpha = 0$  the two tetrahedra are placed face to face sharing the base triangles.

If  $h$  denotes the altitude of the two pyramids, then follows from the proportion  $h : (h - 2h_\alpha) = 1 : \rho$

$$h_\alpha = h \cdot \bar{\rho}, \quad (2)$$

and furtheron with  $t := \tan \alpha$  the algebraic expression

$$h_\alpha(t) = h \frac{t(2\sqrt{3} - t)}{2(1 + 2\sqrt{3}t - t^2)}, \quad 0 \leq t \leq \sqrt{3}. \quad (3)$$

The trajectory  $c_{A_1}$  of  $A_1$  has the cylinder coordinates  $(1, \alpha, -h_\alpha(t))$  by (3).

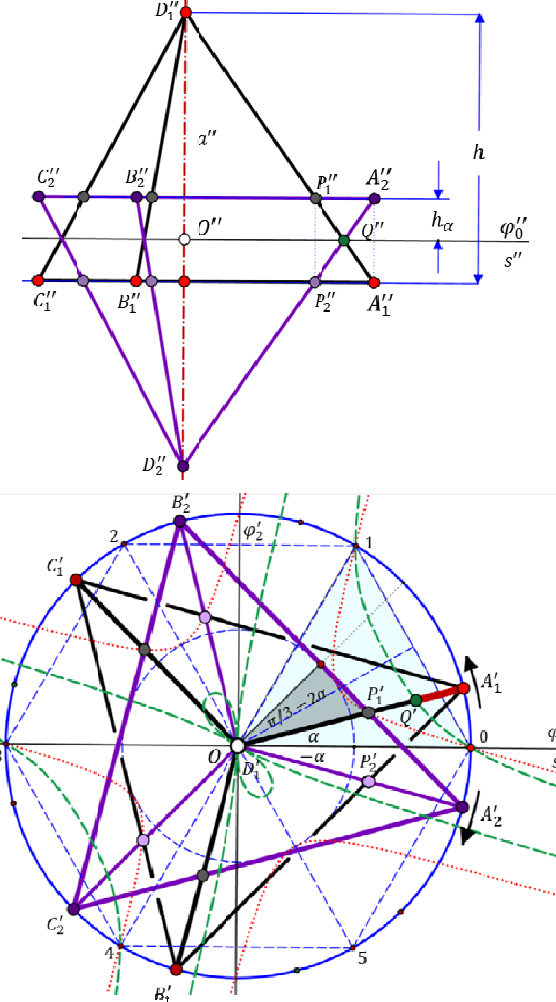


Figure 3: *Front- and top-view of the right pyramids  $T_1$  and  $T_2$  from Figure 2. Here both,  $T_1$  and  $T_2$ , translate symmetric to the plane  $\varphi_0$  along  $a$  through  $h_\alpha$ , while rotating about  $a$  in opposite directions through  $\alpha$ . The top-view (bottom) shows the images of the paths of the contact points  $P_1$  (red) and  $Q$  (green) without restriction to the parameter interval  $0 \leq \alpha \leq \pi/3$ .*

**Theorem 2** *Two congruent right three-sided pyramids  $T_1$  and  $T_2$  admit a one-parameter relative motion with six permanent crossings while the axes of symmetry of the two pyramids coincide.*

**Remark 3** *Since in each pose the pyramid  $T_1$  is symmetric to  $T_2$  w.r.t. the axis  $s = \varphi_0 \cap \varphi_1$ , the relative motion  $T_2/T_1$  is a symmetric roll-sliding as studied by J. Krames in [7]. The locus of  $s$  relative to  $T_1$ , called base surface, is the right conoid defined by the equation  $z = h_\alpha(\alpha)$  according to eqs. (2) and (1).*

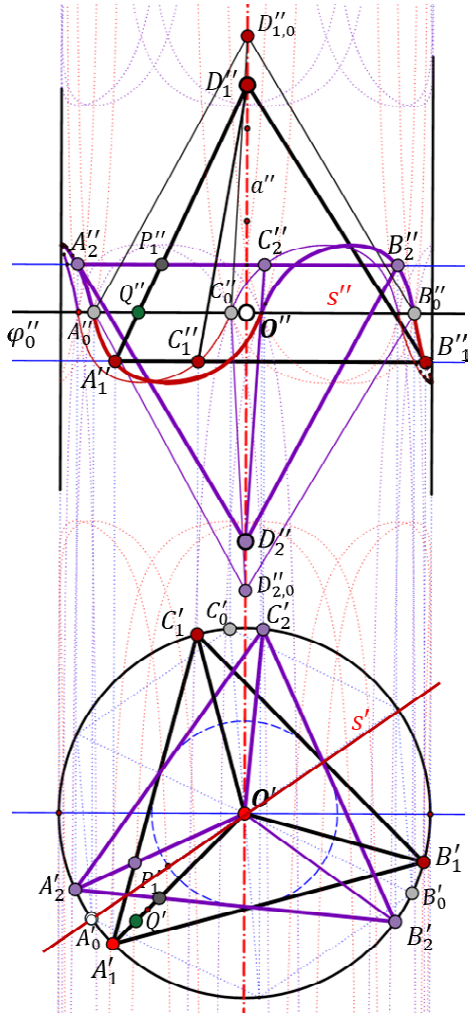


Figure 4: Top- and front-view of intermediate positions of the right pyramids  $T_1$  and  $T_2$ , together with the trajectories of the vertices of  $T_1$  and  $T_2$ , shown as formally closed curves on the unit cylinder with axis  $a$  (red: paths of vertices of  $T_1$ , purple: paths of vertices of  $T_2$ ).

In each pose, the reflection in  $s$  exchanges  $T_1$  and  $T_2$ . Therefore,  $s$  is also an axis of symmetry of the octahedron  $O = T_1 \cap T_2$  with vertices at the contact points (see Figure 2). This symmetry exchanges in particular the regular triangles, along which each tetrahedron intersects the base of the other and which is inscribed in this base.

If the tetrahedra  $T_1$  and  $T_2$  are regular, then we have four possibilities to choose an axis  $a$  and a fixed plane  $\varphi_0$  for performing the one-parameter motion described above. So the question arises, whether these in fact independent motions can be embedded in a two-parameter motion. However, according to [11] this is not the case.

#### 4 Stellae Octangulae formed by equifaced tetrahedra

Now the initial Stella Octangula is formed by the two tetrahedra  $T_1$  and  $T_2$  that can be inscribed in a rectangular box  $\mathcal{H}$  (Figure 5, top). This case was also extensively studied in [8].

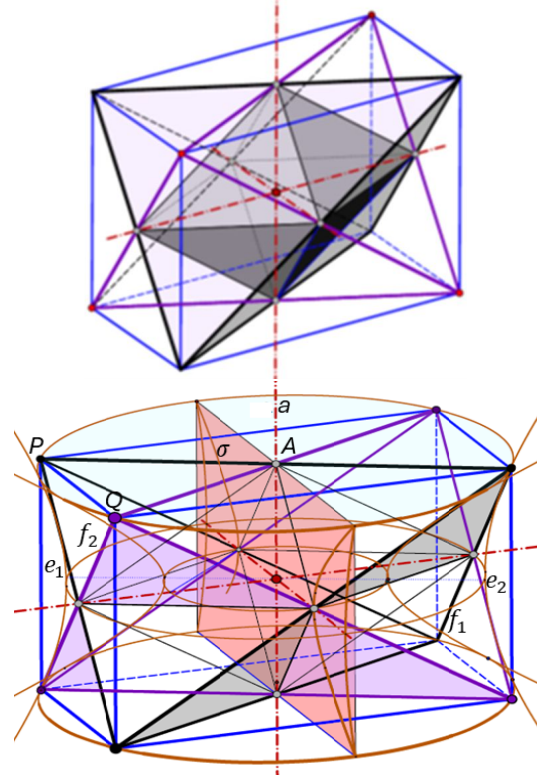


Figure 5: The Stella Octangula based on equifaced tetrahedra  $T_1$  and  $T_2$  has a rectangular box as convex hull (top). The contact points form an equifaced octahedron. Edges of  $T_1$  that are skew to the vertical diameter  $a$  are generators of two hyperboloids of revolution with axis  $a$ .

The two tetrahedra are *equifaced* (or *isosceles*), i.e., all faces are congruent (see, e.g., [5]). The reflection in the center  $O$  of  $\mathcal{H}$  as well as the reflections in a diameter plane  $\sigma$  parallel to one face of  $\mathcal{H}$  exchanges  $T_1$  and  $T_2$  (Figure 5, bottom). Every edge of  $T_1$  has a parallel counterpart at  $T_2$ . Reflections in the three mutually orthogonal axes of symmetry of the box  $\mathcal{H}$  send each tetrahedron onto itself.

The convex octahedron  $O = T_1 \cap T_2$  is equifaced with diagonals parallel to the edges of the box  $\mathcal{H}$ . We keep one diagonal  $a$  of  $O$  fixed and assume that  $a$  is vertical as shown in Figure 5, bottom. Now we focus on the quadrangle of edges of  $T_1$  that are skew to  $a$ .

Two extended opposite edges of this quadrangle are generators of the same regulus of a hyperboloid of revolution  $\Phi_1$  with the axis  $a$ . The other pair of edges defines a second coaxial hyperboloid of revolution  $\Phi_2$ . If we reflect  $T_1$  in any plane  $\sigma$  through  $a$ , then  $\Phi_1$  and  $\Phi_2$  remain fixed while the two reguli are exchanged. The tetrahedron  $T_1$  is sent to a pose  $T_2$ , where each extended edge of  $T_2$  intersects an extended edge of  $T_1$ . Two of these edge-contacts are fixed on  $a$ ; the other four are intersections between generators of different reguli of one of the hyperboloids.

For a suitably chosen  $\sigma$  all intersection points are indeed inner points of the edges. Thereby “suitably” means that the plane  $\sigma$  through  $a$  must be chosen within a restricted angle-interval to ensure that it intersects the edges at inner points. For example, in Figure 5, bottom, this angle interval equals  $\angle PAQ$ , provided that  $PQ$  is a shorter side in the top rectangle of  $\mathcal{H}$ . If  $T_1$  remains fixed while  $\sigma$  rotates around  $a$  within that angle interval, then  $T_2$  performs a continuous rotation about  $a$ .

Since there are three possibilities to choose the axis  $a$ , we can recall from [8]:

**Theorem 3** *The Stella Octangula based on equifaced tetrahedra  $T_1, T_2$  allows three one-parameter motions of  $T_2$  against  $T_1$  that preserve the six crossings. The relative motions  $T_2/T_1$  are terminated rotations about the common perpendiculars of opposite edges of  $T_1$ .*

In the initial position, the octahedron  $O$  of contact points is centrally symmetric with mutually orthogonal diagonals (see Figure 5, top). In the other poses  $O$  has a pair of skew, but mutually orthogonal horizontal diagonals. They are orthogonally intersected by the axis  $a$  being the third diagonal (see Figure 6). Note that parallels of these diagonals through the center  $O$  are the axes of line reflections that exchange  $T_1$  with  $T_2$ .

Can we generalize the statement of Theorem 3? Can also other lines  $a$  through the center of the box  $\mathcal{H}$  serve as axes of rotations that preserve the six edge-contacts between  $T_1$  and  $T_2$  in the Stella-Octangula pose?

Two parallel lines are generators of a one-sheeted hyperboloid of revolution with axis  $a$  if and only if there is a common perpendicular that intersects  $a$  orthogonally in the middle between the two lines. Parallel edges of the two tetrahedra are located in opposite faces of the box  $\mathcal{H}$ , and the common perpendiculars of the edges are parallel to an axis of symmetry of the box. This implies that the axis  $a$  of any rotation in question must coincide with one axis of symmetry of  $\mathcal{H}$ , and one of the three hyperboloids degenerates in two pencils of lines. In other words, there are no other axes of rotations passing through the center of the box.

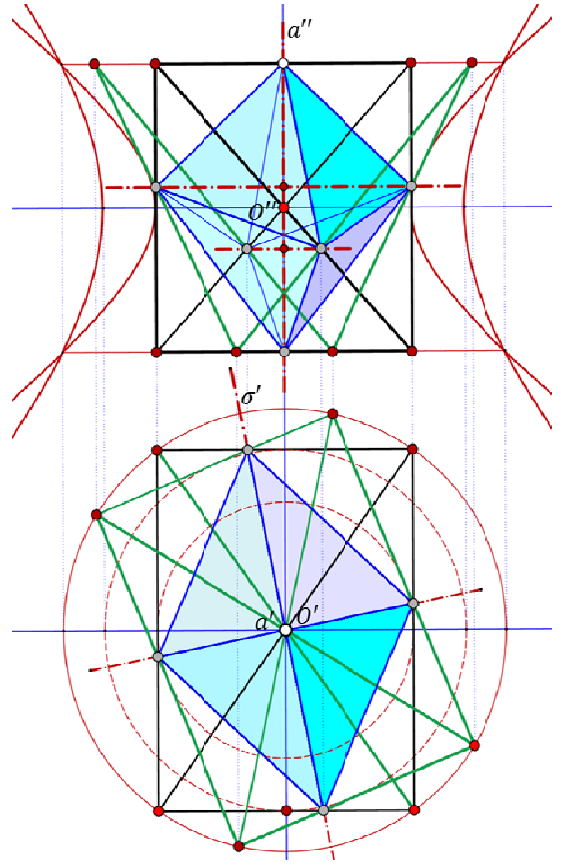


Figure 6: Front view (top) and top view (bottom) of two equifaced tetrahedra  $T_1$  (black) and  $T_2$  (green) with crossing edges. The octahedron of contact points has a pair of skew orthogonal diagonals with the common perpendicular  $a$  as third diagonal. Only in the initial pose the octahedron is centrally symmetric, and all diagonals pass through the center.

The coming Section 5 will reveal that, contrary to Section 3, the three rotations mentioned in Theorem 3 are included in two-parameter motions which preserve all edge-contacts. Moreover, according to Theorem 5 and in agreement with [8], these two-parameter motions contain infinitely many rotations about axes that no longer pass through the center  $O$  of the box  $\mathcal{H}$ .

## 5 Stellae Octangulae formed by tetrahedra with acute-angled faces

Now we consider the general case of a Stella Octangula, where a tetrahedron  $T_1$  is mapped to  $T_2$  by reflection in the barycenter  $O$  of  $T_1$ . Consequently, the two tetrahedra  $T_1$  and  $T_2$  share the midpoints of their edges. We aim at other positions of  $T_2$  having crossing edges with  $T_1$  and obtained by a reflection in a plane  $\sigma$ . Since a plane cannot meet more

than four edges of  $T_1$  at inner points, edge-contacts at two additional points away from  $\sigma$  are necessary.

In the following we explain this for a given sextuple of lines  $\mathcal{L}_1 = (a_1, b_1, \dots, f_1)$ . We choose a pair of points  $P \in e_1$  and  $Q \in f_1$  and their bisecting plane as reflection plane  $\sigma$  (see Figure 7). Then, the reflection of all six lines of  $\mathcal{L}_1$  in  $\sigma$  yields a new sextuple  $\mathcal{L}_2 = (a_2, b_2, \dots, f_2)$ , which is indirectly congruent to  $\mathcal{L}_1$ . Obviously, each line of  $\mathcal{L}_1$  meets its image in the plane  $\sigma$ . However, in addition the image  $e_2$  of  $e_1$  passes through  $Q \in f_1$  and, vice versa,  $f_2$  meets  $e_1$  at  $P$ .

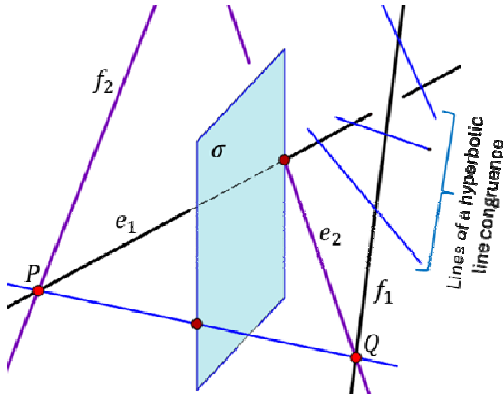


Figure 7: After reflecting a sextuple of lines  $\mathcal{L}_1$  in the symmetry plane  $\sigma$  of two arbitrary points  $P \in e_1$  and  $Q \in f_1$  we obtain an indirect congruent sextuple  $\mathcal{L}_2$  and two additional intersections at  $P$  and  $Q$ .

If  $e_1$  and  $f_1$  are skew, we get a two-parameter set of possible lines  $g = PQ$  forming a hyperbolic congruence of lines, and thus a two-parameter set of reflection planes  $\sigma$ . With regard to our goal, we need to make sure that

- (i) the reflection plane  $\sigma$  intersects four edges of  $T_1$  at inner points and
- (ii) the corresponding points  $P, Q$  are inner points of the remaining two edges.

Reflection planes  $\sigma$  satisfying (i) and (ii) are called *admissible*.

If the six lines of  $\mathcal{L}_1$  are the extended edges of the tetrahedron  $T_1$  and if the bisecting plane  $\sigma$  of two points  $P$  and  $Q$  is admissible, then there exists in a neighbourhood a two-dimensional domain of congruence lines  $g = PQ$  and of admissible reflection planes  $\sigma$ . We will consider the envelope of these planes in Section 5.1.

At a general Stella Octangula, the points of contact between  $T_1$  and  $T_2$  are midpoints of the edges. They form three parallelograms with sides parallel to pairs of opposite edges of  $T_1$  and  $T_2$ . There is a central symmetry between  $T_1$  and  $T_2$ , but in general no planar symmetry like at the equifaced case of Section 4. In general, the octahedron  $O$  of contact points has no mutually orthogonal diagonals (see Figure 8).

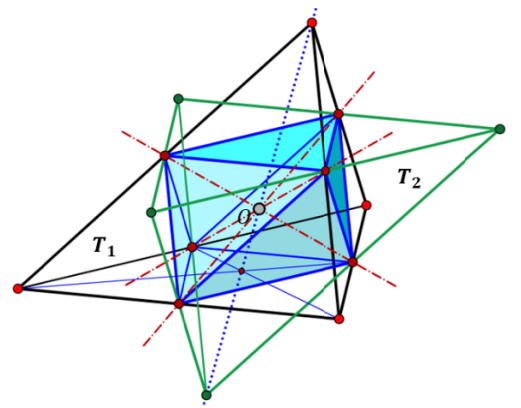


Figure 8: At a Stella Octangula with general tetrahedra  $T_1$ ,  $T_2$  the octahedron  $O$  of contact points is centrally symmetric, and its diagonals are not mutually orthogonal.

Each plane of a diagonal parallelogram is parallel to a pair of opposite edges of  $T_1$ . This means that also the common normal  $n$  of a pair of extended opposite edges  $(e_1, f_1)$  has foot points  $(P, Q)$  symmetric to the corresponding plane (see Figure 9). Therefore, there exists a certain open two-parameter neighborhood of these foot points and thus a two-dimensional manifold of planes  $\sigma$ , where the contact restrictions (i) are fulfilled. One must only make sure that (ii) both foot points  $(P, Q)$  are inner points of the corresponding edges. The contrary situation, where one foot point lies outside, is shown in Figure 10. The following theorem presents a sufficient condition.

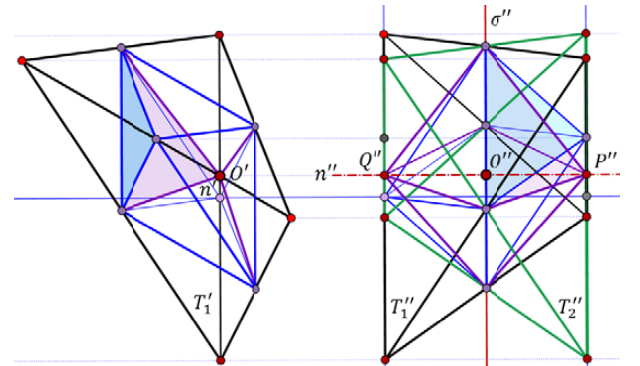


Figure 9: Front view (left) and side-view (right) of a general tetrahedron  $T_1$ , whereby four coplanar midpoints of edges span the projection plane  $\sigma$  for the front view. The reflection in  $\sigma$  transforms  $T_1$  (black) in a tetrahedron  $T'_2$  (green) that in general is different from the centrally symmetric  $T_2$  forming the Stella Octangula.

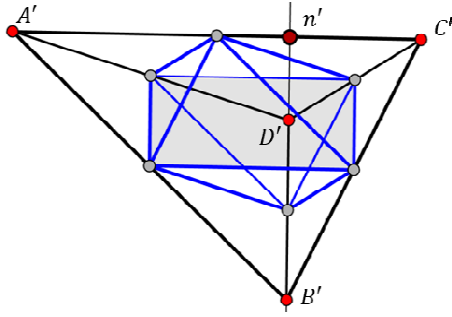


Figure 10: Top-view of a general tetrahedron  $T_1$  with a pair of opposite edges  $[AC]$  and  $[BD]$  parallel to the projection plane  $\sigma$  which contains the parallelogram of midpoints (shaded) of the other four edges. Since the common normal  $n \perp \sigma$  of  $e_1 = AC$  and  $f_1 = BD$  intersects  $[BD]$  at an exterior point,  $T_1$  has obtuse angled faces. Reflecting  $T_1$  in  $\sigma$  gives a tetrahedron  $T_2$ , where the image  $f_2$  of  $f_1$  intersects  $e_1$  in an exterior point.

**Theorem 4** Each tetrahedron  $T_1$  with only acute-angled faces allows three two-parameter motions  $T_2/T_1$  preserving six edge-contacts. In each of the three motions the poses of  $T_2$  arise from  $T_1$  by reflections in a two-parameter set of planes  $\sigma$ . In general, the three motions have no pose of  $T_2$  in common.

**Proof.** We assume that the edges  $[A_1C_1]$  and  $[B_1D_1]$  of  $T_1$  are horizontal. This means for the top view that these edges are parallel to the projection plane. The interior of  $T_1$  should lie under the face  $A_1B_1C_1$ . Then the convexity of  $T_1$  implies that in the top view the signed angle between  $C'_1A'_1$  and  $B'_1D'_1$  lies between  $0^\circ$  and  $180^\circ$ . Let  $n$  denote the common perpendicular of the lines  $A_1C_1$  and  $B_1D_1$ , and suppose that its top view  $n'$  lies outside the segment  $[A'_1C'_1]$ , but closer to  $A'_1$  than to  $C'_1$  (Figure 11, left).

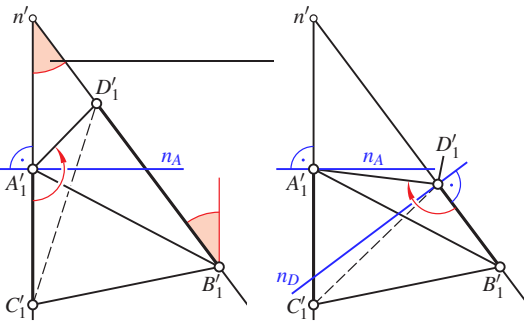


Figure 11: Illustrating the proof of Theorem 4.

If the line  $n_A$  through  $A'_1$  normal to  $A'_1C'_1$  separates  $C'_1$  from  $D'_1$ , then the angle  $\angle C'_1A'_1D'_1$  is greater than  $90^\circ$ . Consequently, also in space the angle  $\angle C_1A_1D_1$  is obtuse.

In the remaining case  $n_A$  separates  $B'_1, D'_1$  and  $C'_1$  from  $n'$ . Then the line  $n_D$  through  $D'_1$  orthogonal to  $B'_1D'_1$  separates  $A'_1$  from  $B'_1$  (Figure 11, right). This implies that the angle  $\angle A_1D_1B_1$  is obtuse. In other words: If one pedal point of a common normal between opposite edges lies on the extension of an edge, then the tetrahedron must have an obtuse-angled face.  $\square$

**Remark 4** The condition of acute-angled faces in Theorem 4 is sufficient, but not necessary since there exist tetrahedra with an obtuse-angled face which nevertheless has the pedal points of the normals between opposite edges inside the edges. This holds, e.g., for the tetrahedron with vertices

$$A = (-0.0, 0.0, 1.0), C = (2.0, 0.00, 1.0), \\ B = (-0.3, 1.0, 0.0), D = (0.3, -0.48, 0.0).$$

We obtain as pedal points of the common normal between opposite edges

$$AC \text{ and } BD : (0.105, 0.000, 1.000), (0.105, 0.000, 0.000), \\ AB \text{ and } CD : (-0.041, 0.136, 0.864), (0.539, -0.412, 0.141), \\ DA \text{ and } BC : (0.112, -0.180, 0.626), (0.569, 0.622, 0.378).$$

Apparently, the first two points are inner points of the edges  $[AC]$  and  $[BD]$ , and the latter four points have  $z$ -coordinates between 0 and 1. However, there is an obtuse angle  $\angle CAB = 101.98^\circ$ . Moreover it needs to be mentioned that for the existence of admissible planes  $\sigma$  for a given pair opposite edges it is not even necessary that the bisecting plane of the foot points of the common perpendicular intersects the remaining edges at inner points (note Remark 6). A necessary and sufficient condition for the existence of the two-parameter motion can be found below in Theorem 6.

Note that for obtaining a standard Stella-Octangula, the reflection of any tetrahedron  $T_1$  in its barycenter produces its mate  $T_2$ . The two-parameter motions discussed in Theorem 4 need another initial pose  $T'_2$ : the acute-angled  $T_1$  is reflected in a plane  $\mu$  through four coplanar midpoints of edges, and there exist three possibilities.

**Lemma 3** Referring to the previous notation, all three initial poses  $T'_2$  of the two-parameter movements coincide with the Stella-Octangula pose  $T_2$  if and only if  $T_1$  is equifaced.

**Proof.** For equifaced tetrahedra holds  $T'_2 = T_2$  as shown in Figure 5, bottom.

Suppose that conversely both the point reflection in the barycenter of  $T_1$  as well as the reflection in the plane  $\sigma$  passing through the midpoints of all line segments  $[PQ]$  with  $P \in [A_1C_1]$  and  $Q \in [B_1D_1]$ , take  $T_1$  to  $T'_2$ . Since the barycenter as midpoint between the midpoints of  $A_1C_1$  and  $B_1D_1$  belongs to  $\sigma$ , the product of the two reflections

is the reflection in the line  $a$  through the barycenter and orthogonal to  $\sigma$ . This product must transform  $T_1$  onto itself. Hence, the halfturn about  $a$  exchanges  $A_1$  with  $C_1$  and  $B_1$  with  $D_1$ , so that we obtain equal lengths  $\overline{A_1B_1} = \overline{C_1D_1}$  and  $\overline{A_1D_1} = \overline{C_1B_1}$ .

If the same assumption holds for another pair  $([A_1B_1], [C_1D_1])$  of opposite edges, then also the last two opposite edges have equal lengths  $\overline{A_1C_1} = \overline{B_1D_1}$ . In other words, the tetrahedron  $T_1$  is equifaced.  $\square$

Lemma 3 means, that only in the particular case of equifacial tetrahedra there exists a single bifurcation between all three two-parameter movements, namely at the common Stella-Octangula pose.

### 5.1 The role of the bisecting paraboloids

In [8], the authors already proved that equifacial tetrahedra with crossing edges admit infinitely many continuous rotations that preserve the edge-contacts. The following generalization for the generic case describes also the geometric loci of the axes of these rotations.

**Theorem 5** *Referring to Theorem 4, for each of the three two-parameter motions  $T_2/T_1$  the admissible reflection planes  $\sigma$  are tangent to an orthogonal hyperbolic paraboloid  $\Psi_1$ , the bisector of the extensions  $e_1, f_1$  of opposite edges of  $T_1$  (Figure 12). Each of these continuous motions includes two one-parameter families of bounded rotations. The axes of these continuous rotations of  $T_2$  against  $T_1$  are generators of  $\Psi_1$  and at the same time axes of rotations that send  $e_1$  to  $f_1$ .*

**Proof.** The symmetry planes  $\sigma$  of all pairs of points  $P \in e_1$  and  $Q \in f_1$  envelop an orthogonal hyperbolic paraboloid  $\Psi_1$ , the bisector of the pair of lines  $(e_1, f_1)$  (see, e.g., [9, p. 64]). Each plane  $\sigma$  contains two generators  $p$  and  $\bar{p}$  of  $\Psi_1$ . Keeping one of these generators fixed, say  $p$ , the tangent planes of  $\Psi_1$  along  $p$  form a pencil. Since the product of the reflections in two planes through  $p$  is a rotation about  $p$ , the admissible planes  $\sigma$  through  $p$  correspond to poses of the tetrahedron  $T_2$  which are related by rotations about  $p$ . According to [9, p. 64], the lines  $p$  on the bisector  $\Psi_1$  are the axes of rotations that send  $e_1$  to  $f_1$ . This agrees with previous arguments, since  $p$  is the axis of a hyperboloid of revolution through  $e_1$  and  $f_1$ , and the reflection in a meridian plane exchanges the reguli. The generators  $p$  and  $\bar{p}$  in the bisecting plane  $\sigma$  of  $P \in e_1$  and  $Q \in f_1$  are axes of rotations that take in addition  $P$  to  $Q$ .  $\square$

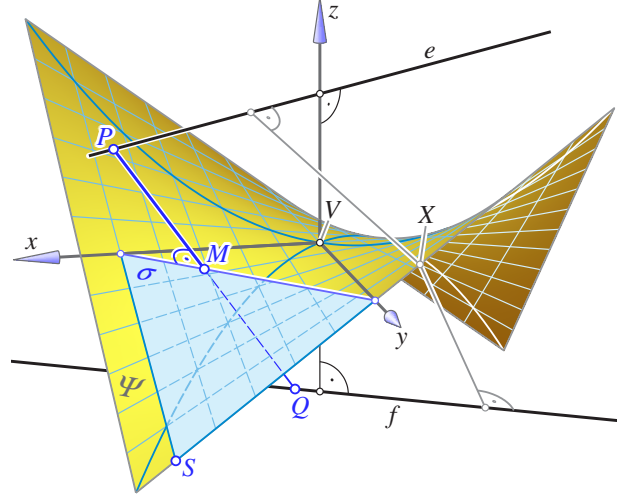


Figure 12: The orthogonal hyperbolic paraboloid  $\Psi$  is the bisector of the skew lines  $e$  and  $f$ , i.e., the set of points  $X$  satisfying  $\overline{Xe} = \overline{Xf}$ . The plane  $\sigma$  of symmetry of the points  $P \in e$  and  $Q \in f$  contacts  $\Psi$  at the point  $S$ .

**Remark 5** *The two-parameter motions according to Theorem 4 are symmetric rollings since an orthogonal hyperbolic paraboloid  $\Psi_2$  attached to  $T_2$  is rolling<sup>2</sup> on an indirectly congruent paraboloid  $\Psi_1$  such that the two surfaces are permanently symmetric w.r.t. the common tangent plane  $\sigma$  at the point of contact. Note the difference: At the symmetric roll-slidings mentioned in Remark 3 the two base surfaces are directly congruent.*

In the particular case of equifacial tetrahedra, the vertex generators of the three bisecting hyperbolic paraboloids are parallel to the edges of the convex hull  $\mathcal{H}$  in the Stella-Octangula pose, i.e., of a rectangular box (see Figure 5, top). The rotations about these particular generators are exactly the same as studied in Section 4.

## 6 The boundaries for admissible reflection planes

A generic plane  $\sigma$  that meets the interior of the tetrahedron  $T_1$  without passing through any vertex, separates either one vertex from the other three or two from two. In the first case we speak of *type-1 planes*, otherwise from *type-2 planes* (see Figure 13). Only type-2 planes are candidates for admissible planes as they meet four edges. We are going to determine the boundaries for the set of admissible planes.

<sup>2</sup>In fact, a rolling of physical models of the paraboloids is not possible since the two surfaces penetrate each other along the common generators in the plane of contact (see Figure 12).

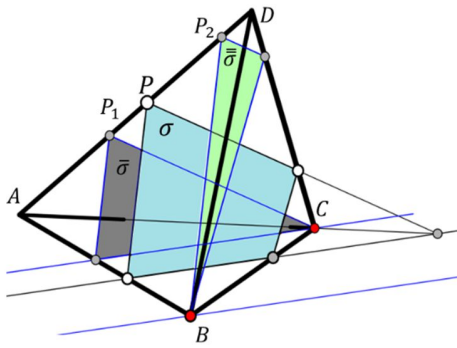


Figure 13: When intersecting a tetrahedron with parallel planes, one finds two open regions where the intersection is empty, two regions of type-1 planes, and one of type-2 planes.

At a given tetrahedron  $T$  (we suppress the subscripts for a while) with vertices  $A, B, C, D$  let  $P \in [AC]$  and  $Q \in [BD]$  be interior points of their edges. Then their midpoint  $M$  on  $g = PQ$  is an inner point of  $T$ . All possible points  $M$  form the interior of an parallelogram in a plane  $\mu$  with the midpoints of the edges  $[AB], [BC], [CD],$  and  $[DA]$  as vertices (see Figure 14).

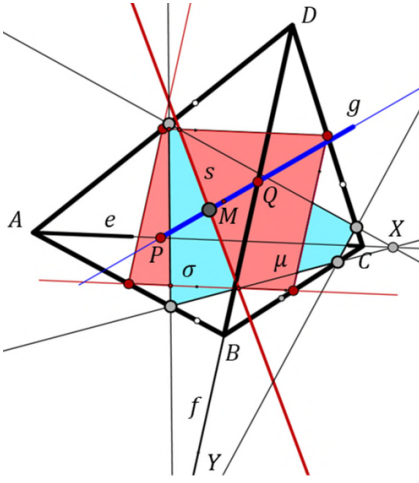


Figure 14: Segments  $PQ$  with their endpoints on opposite edges  $[AC]$  and  $[BD]$  of the tetrahedron  $T$  have their midpoint  $M$  in the plane  $\mu$  parallel to the lines  $e = AC$  and  $f = BD$ . A presumptive reflection plane  $\sigma$  is normal to  $g = PQ$  and contains  $M$ .

Now we intersect the plane  $\sigma$  through  $M$  orthogonal to  $g$  with the extended edges  $e = AC$  and  $f = BD$ . If these intersections are external points, then  $\sigma$  is a type-2 plane as it intersects all sides of the skew quadrangle  $ABCD$  at inner points thus satisfying condition (i). In order to satisfy (ii), the midpoint  $M$  of  $[PQ]$  must be an interior point of the parallelogram  $T \cap \mu$ . We summarize:

**Theorem 6** Let the lines  $e$  and  $f$  be the extensions of opposite edges  $[AC]$  and  $[BD]$  of the tetrahedron  $T$ , and let  $\Psi$  be the bisecting orthogonal hyperbolic paraboloid of  $e$  and  $f$ . Then the set of contact points  $S$  of  $\Psi$  with admissible planes  $\sigma$  related to the edges  $[AC]$  and  $[BD]$  equals the interior of the intersection of two open domains of  $\Psi$ ,

- the domain enclosed by four conics, the contact curves of the tangent cones of  $\Psi$  with apices  $A, B, C, D$ , and
- the domain that results from planes  $\sigma$  corresponding to midpoints  $M$  in the parallelogram  $\mu \cap T_1$  (Figure 15).

For visualizing the two domains, we assume the lines  $e$  and  $f$  along with the plane  $\mu$  to be horizontal and inspect the top view. Note that  $\mu$  is tangent to the hyperbolic paraboloid  $\Psi$  at its vertex  $V$ , and the generators through  $V$  are axes of symmetry of  $e$  and  $f$ . Moreover, according to [9, p. 64] the lines  $e$  and  $f$  are polar w.r.t.  $\Psi$ . Therefore, the tangent cones from  $A, C \in e$  contact  $\Psi$  in the respective polar planes passing through  $f$  and, vice versa, the contact curves for  $B, D \in f$  lie in planes through  $e$ . These four planes enclose the tetrahedron  $T^*$  that is  $\Psi$ -polar to  $T$ . The first domain mentioned in Theorem 6 and corresponding to the condition (i) is the intersection of  $\Psi$  with the interior of  $T^*$  (see Figure 15). In general, it is bounded by four hyperbolic arcs.

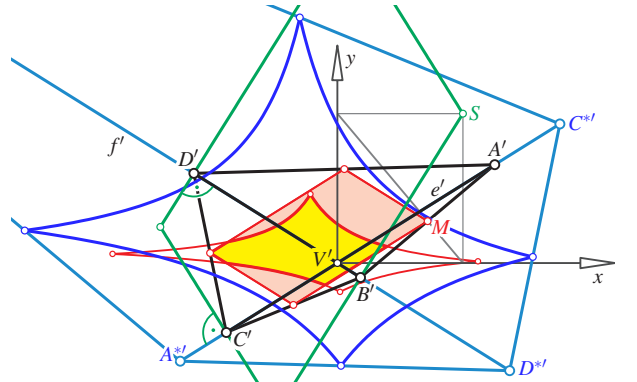


Figure 15: Top views of the tetrahedron  $T$  (black) with the parallelogram of midpoints  $M$  (red), the polar tetrahedron  $T^*$  with vertices  $A^*, \dots, D^*$  (blue) and the four hyperbolic arcs (red) that enclose the first domain of the hyperbolic paraboloid  $\Psi$  as mentioned in Theorem 6. For admissible planes  $\sigma$  the midpoint  $M$  has to be chosen in the yellow area. The green parallelogram is the top view of the four parabolas terminating the second domain for the contact points  $S$  with  $\Psi$ .

For determining the second domain, we choose the generators through the vertex  $V$  of  $\Psi$  as  $x$ - and  $y$ -axis of a coordinate frame and define  $e$  and  $f$  by

$$z = \pm d \quad \text{and} \quad x \sin \alpha = \pm y \cos \alpha,$$

where  $2\alpha = \angle ef$ , and  $2d$  equals the orthogonal distance between  $e$  and  $f$ . This implies

$$\Psi: 2dz + xy \sin 2\alpha = 0.$$

The polar plane of any point  $P = (\xi, \eta, \zeta)$  w.r.t.  $\Psi$  satisfies

$$(\eta x + \xi y) \sin \alpha \cos \alpha + dz = -d\zeta. \quad (4)$$

The vertices  $A^*, C^* \in e$  and  $B^*, D^* \in f$  of the polar tetrahedron  $T^*$  are respectively conjugate to  $A, C, B, D \in T$  w.r.t.  $\Psi$ . Thus, we obtain by (4) for  $A = (a, \text{atan } \alpha, d)$  the vertex  $A^* = (a^*, a^* \tan \alpha, d)$  and for  $B = (b, -b \tan \alpha, -d)$  the vertex  $B^* = (b^*, -b^* \tan \alpha, -d)$ , where

$$aa^* = bb^* = \frac{-d^2}{\sin^2 \alpha}.$$

For describing the second domain, we check the relation between any midpoint  $M \in \mu$  and the contact point  $S$  of the corresponding plane  $\sigma$  with  $\Psi$ :

Given  $M = (\xi, \eta, 0)$ , we first determine the line  $g$  through  $M$  meeting  $e$  and  $f$ . The meeting point  $Q \in f$  is the point of intersection between  $f$  and the plane connecting  $M$  with  $e$ , which satisfies

$$(\xi \sin \alpha - \eta \cos \alpha)(z - d) + d(x \sin \alpha - y \cos \alpha) = 0.$$

This yields

$$\begin{aligned} Q &= (\xi - \eta \cot \alpha, \eta - \xi \tan \alpha, -d) \\ P &= (\xi + \eta \cot \alpha, \eta + \xi \tan \alpha, d). \end{aligned}$$

The bisecting plane of  $P$  and  $Q$  is

$$\sigma: \eta x \cot \alpha + \xi y \tan \alpha + dz = \xi \eta (\tan \alpha + \cot \alpha).$$

We obtain the contact point  $S$  of  $\sigma$  with  $\Psi$  as its pole by comparing the equation of  $\sigma$  with (4) (see Figure 12). This results in

$$S = \left( \frac{\xi}{\cos^2 \alpha}, \frac{\eta}{\sin^2 \alpha}, -\frac{\xi \eta}{d \sin \alpha \cos \alpha} \right). \quad (5)$$

The relation between the top views of  $M$  and  $S$  in the plane  $z = 0$  is affine. Hence, the second domain as locus of admissible points  $S \in \Psi$  as mentioned in Theorem 6 and corresponding to condition (ii) appears in the top view as interior of a parallelogram. It is easy to verify that the side lines of this parallelogram are respectively orthogonal to  $e'$  and  $f'$  and pass through the top views  $A', \dots, D'$  of the vertices of  $T$  (see Figure 15). After transforming the top views of the four hyperbolas by the inverted affine relation  $M \mapsto S$  we find the locus of midpoints  $M$  that correspond to admissible bisecting planes  $\sigma$ .

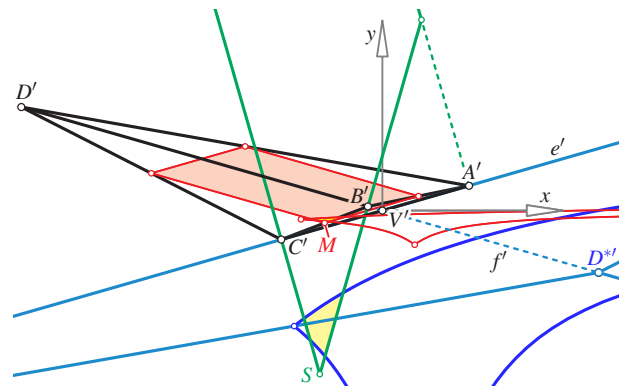


Figure 16: At this example, the common normal of  $e$  and  $f$  (with top view  $V'$ ) has its foot point on  $f$  outside the segment  $[BD]$ . Nevertheless, there exist admissible reflection planes  $\sigma$ . The top views of the domains for the corresponding midpoints  $M$  and for the contact points  $S$  with the hyperbolic paraboloid  $\Psi$  are shaded yellow.

**Remark 6** The example displayed in Figure 16 demonstrates that due to Theorem 6 a two-parameter motion can also exist when the common perpendicular of the opposite edge lines  $e, f$  has a foot point outside the edge. Thus, interior foot points are a sufficient, but not necessary condition for the existence of a two-parameter motion of the type presented in Theorem 4. In other words, along with Remark 4 this means that the tetrahedra with acute-angled faces are a proper subset of the set of tetrahedra where the foot points of all common perpendiculars are interior points of edges. And this is a proper subset of the set of tetrahedra which admit three two-parameter symmetric rollings.

Referring to Figure 16, when the common perpendicular of  $e$  and  $f$  has both footpoints outside the respective edges  $[AC]$  and  $[BD]$ , then the intersection of the two domains mentioned in Theorem 6 must be empty as they are always separated by one coordinate axis.

## 6.1 Contained planar one-parameter motions

A motion in 3-space is called *planar* if all point trajectories are located in parallel planes. For example, according to Theorem 5 all rotations about generators of the bisecting hyperbololic paraboloids are planar motions. There are still more planar one-parameter movements contained in the two-parameter motions of congruent tetrahedra with crossing edges.

We recall that for each pair of opposite edges  $[AC]$  and  $[BD]$  of  $T$  we find admissible reflection planes  $\sigma$  as planes of symmetry for points  $P \in [AC]$  and  $Q \in [BD]$ . If point  $Q$  is kept fixed while  $P$  varies (see Figure 17, top), then the corresponding planes  $\sigma$  envelop a part of a parabolic cylinder. This follows from the standard definition of a parabola

(note, e.g., [2, Fig. 2.13]), since this cylinder intersects the plane  $\gamma$  connecting  $Q$  with  $[AC]$  in an arc of the parabola  $c$  with focus  $Q$  and directrix  $e = AC$  (Figure 17, bottom).

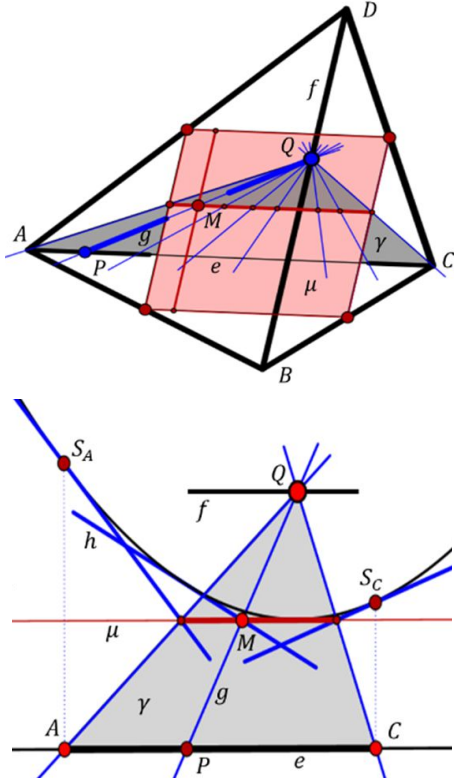


Figure 17: For given opposite edges  $[AC]$  and  $[BD]$  the locus of midpoints  $M$  of points  $P \in [AC]$  and  $Q \in [BD]$  is a parallelogram in a plane  $\mu$  parallel to  $AC$  and  $BD$ . For fixed  $Q$  the planes of symmetry  $\sigma$  envelop a parabolic cylinder.

We are also able to figure out the boundaries of this parabolic arc  $c$  (see Figure 17, top): The plane  $\sigma \perp PQ = g$  passes through the midpoint  $M \in (\mu \cap T)$  of  $[PQ]$  and intersects  $\gamma$  in a tangent  $h$  of  $c$ . The required arc of  $c$  is bounded by the points  $S_A$  and  $S_C$  because of  $P \in [AC]$ . Moreover,  $h \cap e$  has to be an exterior point of the segment  $[AC]$ . Hence, in the case shown in Figure 18, the corresponding parabolic arc is limited by  $S_C$  and by the contact point  $T$  of a tangent  $c$  through  $C$ .

In the limiting case  $Q = B$ , the envelope of the planes  $\sigma$  belongs to a parabolic cylinder with generators orthogonal to the plane spanned by  $ACB$ . These generators have top views orthogonal to the top view  $e'$  of  $e = AC$ . The parabolic cylinder contacts the hyperbolic paraboloid  $\Psi$  along a parabola that bounds the second domain and appears in the top view as a side of the mentioned parallelogram (green in Figure 15). At each point  $S$  of this parabola

the tangent must be conjugate w.r.t.  $\Psi$  to the generator of the contacting cylinder. Conjugate lines are in a harmonic position w.r.t. the  $\Psi$ -generators through  $S$ , which have top views parallel to the coordinate axes. As a result, the top view of the contacting parabola must be orthogonal to  $f'$ , as already documented above (see Figure 15).

When reflecting  $T_1$  on admissible planes  $\sigma$  with fixed point  $Q \in f$  we obtain poses of  $T_2$  where the point attached to  $T_2$  trace curves in planes parallel to the plane  $\gamma$  connecting  $Q$  with  $e$ . At the same time a parabolic cylinder attached to  $T_2$  rolls on a parabolic cylinder attached to  $T_1$  such that the cylinders are permanently symmetric w.r.t. the plane  $\sigma$  of contact. This is again a planar motion contained in the two-parameter motion related to the pair  $(e, f)$ .<sup>3</sup> The corresponding midpoints  $M \in \mu$  trace a segment parallel to  $e$  (Figure 17), hence parallel to one side of the parallelogram in  $\mu$ . The symmetric parabolic-cylinder-rollings corresponding to a fixed point  $P \in e$  has similar properties. In comparison, at the contained rotations according to Theorem 5 the point  $S$  of contact between  $\sigma$  and the paraboloid  $\Psi_1$  (see Figure 12) traces a generator. In the top view, the point  $S'$  runs along a line parallel to one coordinate axis, and the same holds for the midpoint  $M'$  due the affine correspondence between these points (Figure 15).

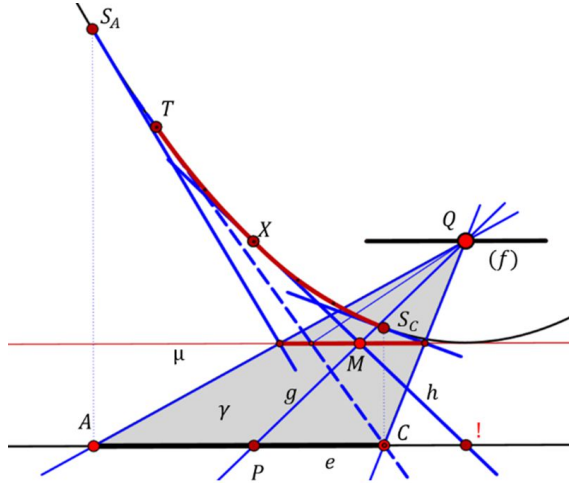


Figure 18: The parabola's tangent at  $S_A$  does no longer belong to an admissible bisection plane  $\sigma$  as it meets the segment  $[AC]$  at an interior point.

## 7 Further movable pairs of congruent structures with edge-contacts

**a)** We follow an idea of [8] generalizing an equifaced tetrahedron with isosceles faces to an antiprisma over a regular

<sup>3</sup>In planar kinematics, the symmetric rolling of two parabolas has the property that the focus of the first parabola traces the directrix of the second parabola while the directrix of the first parabola slides through the focal point of the second.

$n$ -gon (see Figure 19). This allows further generalizations, as we only must demand that the pairs of opposite skew edges of a generalized antiprism are generators of the same coaxial hyperboloid of revolution. Consequently, the regular top- and bottom-polygons can be similar and, to a certain extent, even affine transforms of regular polygons. When we move a planar polygon within its plane to another position, then corresponding edge lines will trivially intersect, and, of course, we can restrict the movement such that all corresponding edges intersect at inner points.

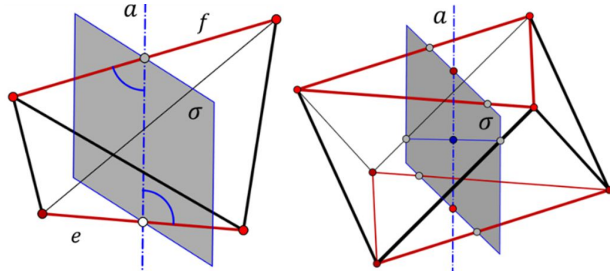


Figure 19: *Pairs of  $n$ -sided antiprisms as movable structures include for  $n = 2$  equifaced tetrahedra (left) and for  $n = 3$  octahedra (right). Also pairs of symmetric tetrahedra with top- and bottom edge of different lengths allow a one-parameter set of motions with fixed axis  $a$ , as well as pairs of generalized antiprisms with affine-regular top- and bottom polygons.*

**b)** When using the last statement for a classical pyramid  $P_1$  with a convex planar basis, then we can, with certain restrictions, reflect it in a plane  $\sigma$  through its altitude  $a$  getting a pyramid  $P_2$ , which is in edge-contact with  $P_1$ . Hence, we can extend an antiprism by two pyramids at the top- and bottom-polygon such that their apices are points of the axis  $a$  of the antiprism. Then the reflection of this polyhedron  $P_1$  in any plane  $\sigma$  through  $a$  yields a congruent copy  $P_2$ , which still can move relative to  $P_1$  while keeping all edge-contacts. For example, a regular icosahedron satisfies these conditions (see Figure 20). A scaling in direction of the axis  $a$  will not restrict the mobility.

**c)** Even congruent pairs of (regular) double pyramids with a non-planar belt-polygon can be considered as movable polyhedral edge structures, as far as the belt polygon also suits to a generalized antiprism. A cube serves as a simple example, when rotated around one of its spatial diagonals. Another example is the regular pentagon dodecahedron, seen as a truncated double pyramid (Figure 21). Obviously the movability remains when such a structure is subjected to a scaling in direction of the fixed axis.

**d)** The standard case of a pair of coaxial right pyramids over a regular  $n$ -gon (see [11] and [12]) allows further generalizations. If  $h$  denotes the altitude of the pyramids and they share in the initial position the base  $n$ -gons, then the extremal distance  $t$  of their base planes is related as

$$t : h = \left(1 - \cos \frac{\pi}{n}\right) : 1. \quad (6)$$

These pyramids  $P_1, P_2$  can be embedded in two congruent cones  $\Psi_1, \Psi_2$  of revolution. When we “bend” all non-base edges of  $P_1$  and  $P_2$  to congruent curves on  $\Psi_1$  and  $\Psi_2$ , then also these objects will allow a one-parameter set of motions as products of appropriate rotations about and translations along the axis, while the formula in (6) will still remain valid.

As a next step we generalize, with restrictions, the cones  $\Psi_1, \Psi_2$  to smooth surfaces of revolution  $\Phi_1, \Phi_2$ . At first we take their meridians  $m$  as replacements of the edges of the pyramids  $P_1, P_2$ . Then again, we can replace these meridians by a set of congruent curves on  $\Phi_1, \Phi_2$ , and we will end up with a movable edge-curve structure.

**e)** We return to **a)** and consider equifaced tetrahedra and regular antiprisms again. There the key property is the existence of coaxial hyperboloids of revolution. Obviously, we can now bend the straight edges to congruent curves on these hyperboloids and receive a movable edge-curve structure. Also here, the hyperboloids can be replaced by more general surfaces of revolution, and, in case of antiprisms, the edges of the top- and base polygon can be replaced by curves, too.

It is easy to imagine such a structure on a sphere: Consider the vertices of a regular  $n$ -gon on, say, the two polar circles of the sphere, and connect them with arcs of, e.g., a loxodrome, a curve of constant slope, or simply with arcs of a great circle. In this very special case of a curved edge system the chosen arcs need not even be congruent.

According to these statements, we can replace the edges of the cube, the regular icosahedron and the pentagon dodecahedron (see **b)** by congruent curves and preserve the movability of the curved edge structure.

Nevertheless, an explicit calculation of the motion will depend on the chosen curved edges and might get lengthy. In each pose, the instantaneous behaviour is that of an object with the tangents as edges, and therefore it is locally an edge structure of the types treated in the foregoing chapters.

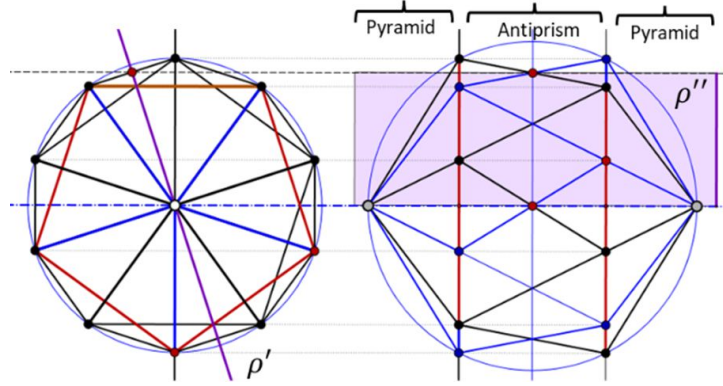


Figure 22: *A regular icosahedron together with its image under a rotation about an axis connecting opposite vertices yields two congruent polyhedral structures which allow a relative movement while all edge-contacts are preserved.*

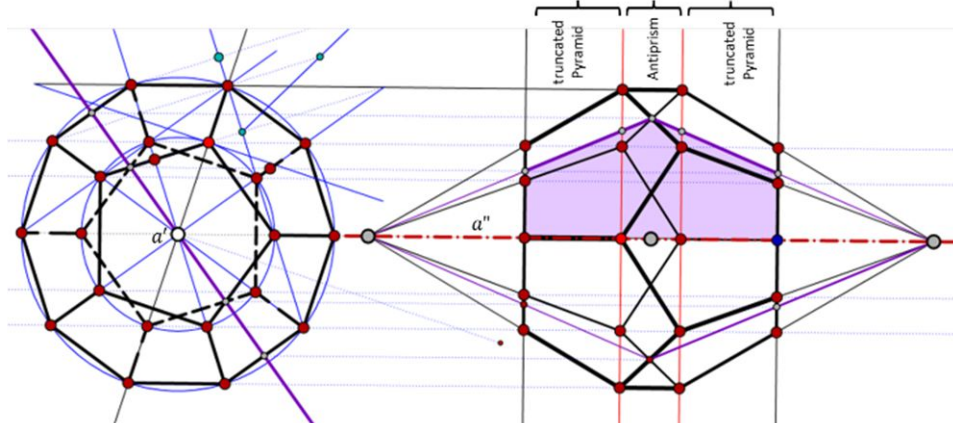


Figure 21: *Another example of a movable polyhedral edge structure consists of two congruent regular pentagon dodecahedra sharing an axis that connects midpoints of opposite faces.*

## 8 Conclusion

We aimed at a geometric analysis of the sliding motions, which occur at congruent tetrahedra, forming a Stella Octangula in the initial pose. We preferred geometric reasoning against lengthy calculations. The surprising fact that the pair of tetrahedra of a classical Stella Octangula is movable in spite of  $\text{dof} = 0$  caused the questions “why” and “are regular tetrahedra the only ones with that property”. We could show that general pairs of indirect congruent tetrahedra ( $T_1, T_2$ ) keep their six crossings under three two-parametric motions of  $T_2$  relative to  $T_1$ . Each pose of  $T_2$  can be obtained by a reflection of  $T_1$  in a tangent plane of orthogonal hyperbolic paraboloids, and their generators act as axes of possible rotations.

There is kind of hierarchical structure among the tetrahedra  $T_1, T_2$  from the most general ones to those having in the initial Stella-Octangula pose a box as convex hull, and

finally those being regular three-sided pyramids. The latter allow motions generated by reflections in axes orthogonal to the common axis of symmetry of  $T_1$  and  $T_2$ . The most special case with two regular tetrahedra allows both, the special axial reflections as well as the reflections in planes. In all the discussed cases, the poses of  $T_2$  relative to  $T_1$  are generated by single reflections, i.e., by involutive displacements. Here the question arises: “Is the assumption of tetrahedra  $T_1, T_2$  being congruent a necessary condition for their movability?”

Moreover, one might ask for pairs of other polyhedral structures, which allow such relative motions. Besides generalizations presented in [8], it is possible to find many other polyhedral structures allowing at least one-parameter motions, if trivial edge-contacts are not excluded. In addition, even structures where the edges are bent to congruent curves can admit such sliding motions.

## References

[1] BOTTEMA, O., ROTH, B., *Theoretical Kinematics*. North-Holland Publ. Comp., Amsterdam, 1979.

[2] GLAESER, G., STACHEL, H., ODEHNAL, B., *The Universe of Conics*. 2<sup>nd</sup> ed., Springer Spektrum, Heidelberg, 2024, <https://doi.org/10.1007/978-3-662-70306-9>

[3] HUSTY, M., KARGER, A., SACHS, H., STEINHILPER, W., *Kinematik und Robotik*. Springer-Verlag, Berlin-Heidelberg, 1997, <https://doi.org/10.1007/978-3-642-59029-0>

[4] HYDER, A., ZSOMBOR-MURRAY, P., An equilateral tetrahedral mechanism. *Robotics and Autonomous Systems* **9**(4) (1992), 227–236, [https://doi.org/10.1016/0921-8890\(92\)90040-6](https://doi.org/10.1016/0921-8890(92)90040-6)

[5] KATSUURA, H., Characterization of an Isosceles Tetrahedron. *J. Geom. Graph.* **23**(1) (2019), 37–40.

[6] KRAMES, J.L., *Darstellende und kinematische Geometrie für Maschinenbauer*. 2nd ed., Franz Deuticke, Wien, 1967.

[7] KRAMES, J., Über Fußpunktkurven von Regelflächen und eine besondere Klasse von Raumbewegungen. (Über symmetrische Schrotungen I). *Monatsh. Math. Phys.* **45** (1937), 394–406.

[8] MAKAI, E., TARNAI, T., Generalized Forms of an Overconstrained Sliding Mechanism Consisting of Two Congruent Tetrahedra. *Stud. Sci. Math. Hung.* **60**(1) (2023), 43–75, <https://doi.org/10.1556/012.2023.01534>

[9] ODEHNAL, B., STACHEL, H., GLAESER, G., *The Universe of Quadrics*. Springer-Verlag, Berlin, Heidelberg, 2020, <https://doi.org/10.1007/978-3-662-61053-4>

[10] QUAISSER, E., *Bewegungen in der Ebene und im Raum*. VEB Deutscher Verlag der Wissenschaften, Berlin, 1983.

[11] STACHEL, H., Ein bewegliches Tetraederpaar. *Elemente der Math.* **43**(3) (1988), 65–75.

[12] TARNAI, T., MAKAI, E., A movable pair of tetrahedra. *Proc. Royal. Soc. London A* **423** (1989), 419–442.

[13] WEISS, G., Symmetry in motion: Stellae Octangulae, and equifaced polyhedra. *Proceedings of “Symmetry: Art and Science”*, 12<sup>th</sup> SIS-Symmetry Congress, Porto 2022, 210–217, <https://doi.org/10.24840/1447-607X/2022/12-26-210>

### Hellmuth Stachel

orcid.org/0000-0001-5300-4978  
e-mail: stachel@dmg.tuwien.ac.at

Vienna University of Technology  
Wiedner Hauptstr. 8-10/104, 1040 Wien, Austria

### Gunter Weiss

orcid.org/0000-0001-9455-9830  
e-mail: weissgunter@gmx.net

Vienna University of Technology  
Wiedner Hauptstr. 8-10/104, 1040 Wien, Austria